Nonlinear effects in desorption of valine with fast incident molecular ions

Mehran Salehpour,* Derry L. Fishel,† and Jerry E. Hunt
Chemistry Division, Argonne National Laboratory, Argonne, Illinois 60439
(Received 17 May 1988)

Fast molecular ions as primary particles have been used to study secondary-ion desorption from organic layers. The secondary molecular-ion yield of the amino acid valine (molecular weight, 117) has been measured as a function of the velocity of primary atomic and molecular incident ions. The primary ions used were C^+, O^+, Ar^+, C_2^+, O_2^+, CO^+, CO_2^+, CH^+, CH_3^+, CF^+, CF_3^+, $C_3F_5^+$, and $C_4F_7^+$ in the energy range 600 keV–3.7 MeV. The secondary molecular-ion yields, when compared to yields for atomic constituents, unambiguously show that collective effects exist in desorption with incident molecular ions. Results are discussed in the framework of enhancement in the electronic stopping power per atom for molecular ions due to the vicinage of the fast-moving charges in the material. The resulting high-yield enhancements, especially with the use of large incident ions such as $C_3F_5^+$ and $C_4F_7^+$, are very encouraging for the future of mass spectrometry of large organic molecules.

I. INTRODUCTION

As energetic particles traverse matter, energy is deposited as a result of collisions with nuclei and electrons. The energy loss per unit path length is referred to as the stopping power which may be divided into two overlapping regions determined by the velocity of the incoming ion. If the incident ion velocity is less than the orbital velocity of its electrons and those in the target, energy loss will be governed by the screened Coulombic collisions of the atoms giving rise to momentum transfer to the solid nuclei. This is referred to as the nuclear stopping power. At higher ion velocities, the electrons in the solid near the ion's path cannot react adiabatically due to the short collision time and, therefore, ion-electron interactions become the main mode of energy loss, the so-called electronic stopping power. A commonly used constant to coarsely separate electronic and nuclear stopping powers for heavy atomic ions (i.e., $Z>3$) is the Bohr velocity ($v_0=0.218$ cm/ns), which is the velocity of the electron in the ground state of the hydrogen atom. In this paper we use the terminology slow and fast ions for ions with velocities lower than and greater than v_0, respectively.

One of the secondary effects caused by incident energetic ions is the ejection of neutral and ionized atoms and molecules from sample surfaces. This is referred to as "sputtering" or "desorption." Since slow and fast ions deposit energy due to different types of interactions, the resulting sputtering effect is also governed by different mechanisms. For slow ions, nuclear sputtering is a result of nuclear collisional cascades caused by the momentum transfer between the incident ion and the atoms in the medium. This has been described theoretically by Sigmund[1] and is directly related to the nuclear stopping power.

In 1974 Macfarlane and co-workers discovered that fragments from fissioning ^{252}Cf nuclei (fast ions), upon impact at organic surfaces, cause ionization and desorption of complex molecules.[2] A time-of-flight technique was employed for secondary-ion mass analysis and the method was named plasma desorption mass spectrometry (PDMS). They showed that this technique could be utilized to mass analyze involatile and thermally labile molecules not possible with other methods at that time.[3] Before this discovery, the upper mass limit for organic molecular ions with a molecular weight (MW) of about 2000. Now, commercial PDMS instruments are available[4] and the phenomenon is being utilized to mass-analyze small proteins such as trypsin[5] (MW of 24 000) and pepsin[6] (MW of 34 000).

An array of experimental data has provided some insights into the mechanism of desorption. For fast ions, the electronic stopping power, dE/dx, has been shown to be responsible for fast-ion-induced desorption,[7,8] the so-called "electronic sputtering." Unlike nuclear sputtering, which applies to metals and insulators, electronic sputtering is only effective in insulators.[9] An experimental parameter often measured and referred to is the molecular yield which is defined as the number of desorbed neutral or ionized molecules per incident ion. Other important findings are (1) The total yield is very high[10] ($\sim$1200 intact molecules for 90-MeV ^{127}I) and ratio of the charged to neutrals is about 10^{-4}, (2) the yield is strongly dependent on the charge state of the incident ion,[11–13] (3) the desorption depth is in the order of 100 Å,[14,15] and (4) Håkansson *et al.*[16] have shown that a minimum stopping power is needed for desorption of very large organic molecular ions. However, the details of the ejection mechanism are not fully understood.

Brandt *et al.*[17] have shown the existence of collective effects in energy deposition of molecular ions in solid carbon. In experiments with H^+, H_2^+, and H_3^+ incident ions, the ratio R of the electronic stopping power of a hydrogen atom in a cluster to that of atomic hydrogen was reported to be higher than 1 (maximum $R\sim1.5$ at 80 keV/nucleon), implying collective effects due to the vicinage of the moving hydrogen atoms. Tape *et al.* later showed the same effect for O_2^- ions in the same velocity range.[18]

The importance of using molecular incident ions in

electronic sputtering is twofold. First, from a mechanistic point-of-view, it is important to study the collective effects of temporally and spatially correlated atoms and the corresponding effect on desorption yields. Second, from an applied point of view, the inherent nonlinearities associated with the stopping power of cluster ions means higher obtainable dE/dx and, thus, the possibility of studying higher-molecular-weight compounds.

For slow incident ions, secondary yield enhancements have been reported for metal clusters on metals.[19–21] There have been two qualitative experiments with incident molecular ions on organic molecules.[22,23] For fast incident ions, Brown *et al.*,[24] for the first time, showed molecular effects in the total yield of water ice with H_2^+ and H_3^+ incident ions. Thomas *et al.* used hydrogen clusters to measure the yield of secondary positive Cs (Ref. 25) and phenylalanine molecular ions[26] as a function of the number of hydrogens in the cluster at a fixed energy. We recently reported the use of fast primary carbon clusters,[27] large hydrocarbon ions[28] such as $C_3H_3^+$, $C_4H_9^+$, and $C_7H_{15}^+$, and also CF_3^+ ions[29] for desorption studies.

We present experimental results for the secondary ion yield of the model compound valine (MW of 117) for a wide variety of incident molecular ions over a range of velocities and compare the results to those of atomic ions. Furthermore, interactions of fast molecular ions with solids and the relationship to nonlinear desorption is discussed.

II. EXPERIMENTAL

The Dynamitron accelerator at the Physics Division, Argonne National Laboratory, has been used as the source of primary atomic and molecular-ion beams. The reliable operating range of the accelerator, considering the ion optics and terminal voltage limitations, is in the range 500 keV–4 MeV for singly charged ions. The ion source is based on low-energy electron bombardment of atoms and molecules in the gas phase. A favorable characteristic of the ion source is its low current output which makes it particularly suitable for single-particle counting techniques. The ion beam is collimated to about 2 mm in diameter by four sets of four-jaw slits. A magnet facilitates momentum analysis of the ion beam before entering the mass spectrometer. The count rate of primary ions in the mass spectrometer is in the range 50–4000 sec^{-1}, depending on the abundance of the particular ion in the ion source.

A surface barrier detector (SBD) is used for particle energy and flux measurements. Incident molecular-ion identification is achieved by energy analysis of molecular fragments utilizing a SBD. The vacuum in the beam line between the magnet and the mass spectrometer is about 1×10^{-6} torr. This is sufficiently high to cause an appreciable number of collisions between the primary molecular ions and the rest gas. This results in fragmentation of the primary molecular ion. The fragments are detected in the SBD with energies determined by the ratio of fragment to parent mass. Therefore, each molecular ion has a signature decomposition energy spectrum. The level of fragmentation is about 1% of the parent ion in our setup which is ideal since it is not large enough to be a serious beam contaminant. Such analysis is especially useful to avoid mistaking molecular ions for atomic ions (e.g., F^+ and H_3O^+).

The time-of-flight mass spectrometer is in a vacuum chamber at a base pressure of about 3×10^{-8} torr. The spectrometer consists of a target holder assembly at high voltage, a complementary acceleration grid setup, a field-free flight path for secondary ions and electrons, a detector for timing measurements, and a surface barrier detector (Fig. 1). The target assembly, which is movable in vacuum and is connected to a high-voltage power supply (0–20 kV, negative), allows loading of five samples simultaneously. The samples are prepared by electrospraying[30] a thick layer of valine on a stainless steel backing or aluminized Mylar films. The sample is positioned at 45° with respect to the primary ion beam. A 90% transmission acceleration grid at ground potential is located 6 mm from the sample surface. In between the target-grid assembly and the secondary-ion detector is a 40-cm-long field-free flight path, which has been grounded and magnetically shielded to eliminate the effect of stray fields on the trajectory of the secondary ions and electrons. This is particularly important for detection of secondary electrons which are used to trigger the start pulse. The secondary ion detector is a tandem coupling of channel electron multiplier plates which gives a fast timing signal output upon impact of an ion.

When a desorption event occurs, the negatively charged species are accelerated towards the grid and then drift in the field-free region. The time-of-flight measurements, recorded by a multihit time-to-digital converter, are thus based on the time differences between the arrival of the fast electrons emitted from the surface and the negatively charged secondary ions sputtered from the sample surface. The secondary molecular-ion yield is the integral of the molecular-ion peak divided by the number of incident ions.

When a fast ion impacts on a sample surface, a large number of secondary electrons are emitted from the sample surface. For the energy range of our experiment, the yield of secondary electrons (number emitted per incident

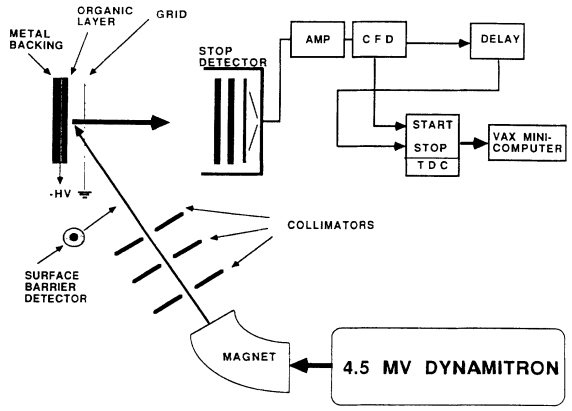

FIG. 1. The schematic diagram of the experimental setup. Abbreviations used are, amplifier (AMP), constant fraction discriminator (CFD), and time-to-digital converter (TDC).

ion) is in the range 20–70 per incident ion,[31] depending on the velocity and the atomic number of the primary ion. The secondary electron shower is used to signal the impact of a primary ion on the surface and thus start the time-of-flight measurements. One start pulse will be registered irrespective of the number of emitted secondary electrons per incident ion. Thus, the secondary-electron pulses can be used to measure the number of incident ions impinging on the sample surface. In order to be able to measure reliable secondary ion yield values, care must be taken in order to assure that all secondary electron showers are detected, i.e., one start pulse is obtained per incident ion. Test experiments were performed where the primary ion rate I was measured with a SBD and the rate was compared to that of secondary electron pulses, Ω, from the sample. The electrons are distinguished from the secondary ion count rate according to the flight times. Because of stray magnetic fields, Ω/I values as low as 10% were initially measured. However, by using μ-metal material to shield the flight path the value was increased to 90% with a standard of deviation of 12% for 47 experiments with primary atomic- and molecular-ion beams of different energies and atomic number. Therefore, a systematic error of about 10% is expected. In all experiments, as a means of additional control, the primary ion count rate was measured before and after each time-of-flight measurement.

Our measurements are limited to negatively charged secondary ions. In conventional accelerator-based electronic sputtering experiments, the primary ion beam passes through the sample (or an electron-emitting foil) and initiates the start signal in a detector for the time-of-flight measurement. However, at the energy range of our experiment, the energy loss in thin targets could be high enough to stop the ion beam. Thin aluminized Mylar films are a convenient sample backing to use in PDMS and high-energy electronic sputtering. A typical beam used in our experiments is 1.5-MeV C^+, which has an estimated stopping power of about 100 eV/Å in Mylar. Even the thinnest Mylar films available commercially, about 200 $\mu g/cm^2$ thick, are thick enough to stop the primary ion beam. A typical fission fragment (e.g., 100 MeV $^{106}Tc^{22+}$), loses only about 15% of its total energy in the same film. Therefore, either very thin samples should be used ($\ll 100$ $\mu g/cm^2$) or the start signal should be obtained in another way, as described above. Concerning the former, we have prepared thin films (5–10 $\mu g/cm^2$) of Formvar, and the energy loss in the film was measured to be small compared to the total beam energy ($\sim 10\%$). However, more experimental work is underway to test for reproducibility and characteristics of such films in vacuum.

Different positions on the targets may be analyzed by the primary ion beam for different measurements which could be a source of error. For a given sample we found that by moving the target over distances greater than the beam spot, reproducibilities of better than 7% are obtained. However, by analyzing the same position on the target (as is the case during experiments) the reproducibility is within the statistical uncertainty (3%) over a period of hours. Over a period of three days the yield varied by no more than 6%. Data points taken more than one day apart were remeasured for such errors.

III. RESULTS AND DISCUSSION

A. Incident atomic ions

One of the characteristic features of fast-particle-induced desorption ionization is the formation of protonated and deprotonated secondary molecular ions, i.e., $(M \pm H)^{\pm}$. All amino acids abide by this empirical rule.[32] Figure 2 shows part of the time-of-flight mass spectrum for the amino acid valine ($C_5H_{11}NO_2$) With 2.5-MeV Ar^+ as the primary incident ions. The molecular ion $(M\text{-}H)^-$ and the fragments $(M\text{-}COOH)^-$ and CN^- are all characteristic of the valine mass spectrum. The peaks at masses 113 and 69 are the molecular ion, $(TFA\text{-}H)^-$, and fragment ion, CF_3^-, from the solvent, trifluoroacetic acid (CF_3COOH), which can also be used for calibration purposes.

The velocity range of the incident ions is between two limits, namely, the velocity of the incident ions' loosely bound valance and K-shell electrons. Thus, according to Bohr's criterion,[33] the valence electrons will be stripped off, whereas the K-shell electrons will respond adiabatically and will not be stripped off the incident ion. In order to estimate the time scale (and hence the depth) in which charge equilibrium is reached, experimental data on the electron-loss cross section is needed. Simple rough estimates made by taking the electron-loss cross section as that of the size of the L shell[34] indicate that within a few angstroms from the surface the L-shell electrons are lost. A large body of experimental results exists on the electron-loss cross section[35] σ_{nm} (i.e., change from charge state n^+ to m^+ with $m > n$). Since the concept of additivity of atomic charge-exchange cross sections for molecular targets is known to be invalid,[36] we do not attempt to do any calculations for valine. The most comparable ion-target combination and energy range to this

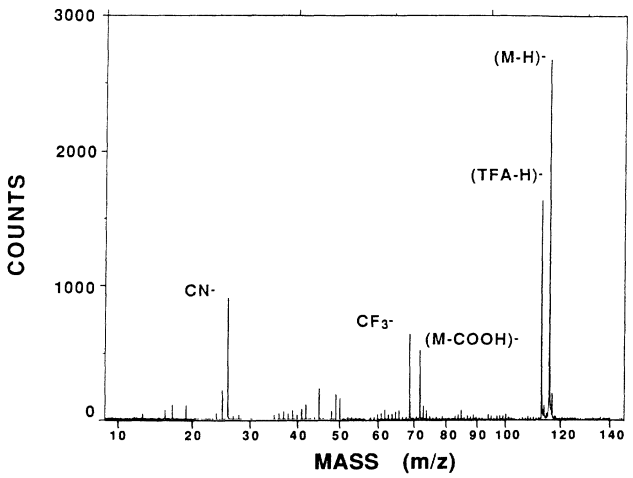

FIG. 2. Time-of-flight mass spectrum for secondary ions from a valine sample with 2.5-MeV Ar^+ incident ions. M denotes the valine molecule and TFA the trifluoroacetic-acid solvent molecule.

experiment is nitrogen ions incident on a target of nitrogen molecules with $\sigma_{12}=0.5$ Å^2 and $\sigma_{23}=0.33$ Å^2 per L-shell electron.[37] Assuming a realistic electron number density such as that of solid carbon ($n=4\times10^{23}$ electrons/cm^3) one calculates that within the first 10 Å there is a very high probability ($>90\%$) of losing the L-shell electrons. This is consistent with the finding of Maor *et al.*[34] for charge equilibration of 2.1-MeV N^+ ions. It should be noted that at higher velocities, where K-shell ionization is possible, much longer equilibrium lengths are predicted and observed.[38] This is because the electron-loss cross sections for K-shell electrons are much smaller than for the L shell and therefore charge equilibration takes a correspondingly longer time.

Measurements of Säwe *et al.* have shown that the depth of desorption, L_d, for valine secondary molecular ions with 6.8-MeV carbon incident ions is of the order of 100 Å.[14,15] Since 6.8-MeV carbon is over the maximum of the electronic stopping power,[39] and our experiments are near the electronic stopping-power maximum, L_d is at least 100 Å in our experiment. Since the equilibration length L_e was estimated to be of the order of a few angstroms, we have $L_e/L_d \ll 1$. Thus, the effect of charge equilibration is expected to have a small effect on desorption yields.

A pertinent parameter in electronic sputtering is the electronic stopping power, dE/dx. Experiments by Håkansson *et al.*[7] and Dück *et al.*[8] have shown that the electronic stopping power dE/dx is directly related to desorption. However, the fraction of the total dE/dx responsible for desorption is unknown. The stopping-power tables of Northcliffe and Schilling[40] are rather inaccurate (up to a few hundred percent) in this energy range.[41] In addition, the dE/dx tables of Ziegler[39] for heavy ions do not cover the energy range in this experiment. Therefore, we use the effective charge concept[42] to scale the electronic stopping powers of ions at the same velocity as protons.[43] The electronic stopping power of an atom with atomic number Z is given by

$$\left.\frac{dE}{dx}(Z)\right|_v = \left.\frac{dE}{dx}(H)\left[\frac{q^2(Z)}{q^2(H)}\right]\right|_v , \tag{1}$$

where $(dE/dx)(H)$ is the electronic stopping power of a proton in the medium at velocity v, calculated using Bragg's rule.[39] Experimental $(dE/dx)(H)$ values have been tabulated in Ref. 43 for atomic targets. The effective charge of the ion in the solid is discussed in detail by Brandt[42] and Betz[44] and is given by the relation

$$q(Z)=Z(1-e^{-[v/(v_0Z^{2/3})]}) . \tag{2}$$

Gaseous argon and carbon dioxide have been introduced to the ion source of the Dynamitron accelerator to produce fast primary ion beams of C^+, O^+, and Ar^+. The yields of valine negative molecular ions Y have been measured as a function of the velocity of incident C^+, O^+, and Ar^+ ions. The corresponding stopping powers have been calculated according to Eqs. (1) and (2) and Ref. 43. Figure 3 shows $Y(M\text{-H})$ as a function of the square of the stopping powers of the incident ions. The linear correlation shows that for incident C^+, O^+, and Ar^+ ions,

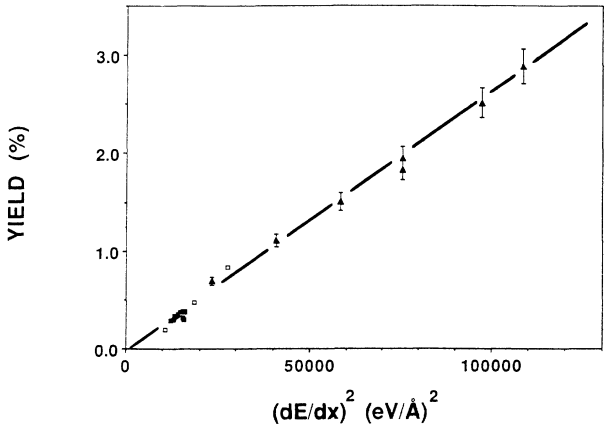

FIG. 3. The yield of valine secondary molecular ions, $(M\text{-H})^-$ as a function of the square of the electronic stopping power of the incident C^+ (solid squares), O^+ (open squares), and Ar^+ (solid triangles) incident ions at different energies.

$$Y(Z)=K\left[\frac{dE}{dx}(Z)\right]^2 , \tag{3}$$

where $Y(Z)$ denotes the secondary molecular-ion yield for an incident ion with atomic number Z and K is a constant, independent of Z. A quadratic yield dependence on the electronic stopping power has also been observed by others.[7,45–48] This relation, however, may not hold for positive secondary molecular ions or at much higher incident ion velocities[46,47] and stopping powers.[16]

B. Incident molecular ions

1. *Coulomb explosion of incident molecular ions*

Once a molecular ion enters the solid, the binding electrons are lost and the nuclear charge is partially exposed. The resulting Coulombic field will cause the constituent atoms to experience a strong Coulomb repulsion. For example, for 1.6-MeV C_2^+, once charge equilibrated, there is approximately 100 eV in repulsive Coulombic energy between the two carbon atoms. Thus, the distance between the atoms increases and the atoms finally separate in the time scale of a few femtoseconds. This is called "Coulomb explosion" of the molecule. The equation of motion has been solved for a diatomic molecule[17] and the results are given below. The incident molecule reaches charge equilibrium very quickly. Thus, two atoms with masses M_1 and M_2 and velocity v are regarded as two point charges with charges equal to the corresponding effective charges q_1 and q_2 [see Eq. (2)] at an initial internuclear distance of r_0 (bond length) and a distance of $r(t)$ thereafter. Solving for a force $F(r)=q_1q_2e^2/r^2$ gives the expression for the depth D of the cluster ion in the solid as a function of the internuclear distance $\zeta=r/r_0$,

$$D=vT_0[\sqrt{\zeta}\sqrt{\zeta-1}+\ln(\sqrt{\zeta}+\sqrt{\zeta-1})] , \tag{4}$$

where $T_0=(\mu r_0^3/2q_1q_2e^2)^{1/2}$ and the reduced mass $\mu=(M_1^{-1}+M_2^{-1})^{-1}$.

Figure 4 shows the internuclear distance $r(t)$ calculated as a function of depth D of the cluster in the solid for C_2^+ and CH^+ clusters at a velocity of 0.54 cm/nsec (i.e., 1.9-MeV CH^+ and 3.5-MeV C_2^+). At depths comparable to the desorption length (~ 100 Å), the internuclear separation is close to r_0, so the Coulomb explosion is still in an early stage. Therefore any collective molecular effects of impinging molecular ions are expected to directly affect the desorption yield. The incident molecular ions were assumed to be in the ground state, however, averaging the internuclear distances over all the vibrational states was found to have a small effect.[17,49] For internuclear distance above the dynamic screening length[49] (i.e., when the target electrons screen the internuclear potential) Eq. (4) is not valid. However, for the discussion above ($D \approx 100$ Å), the internuclear separation is less than the screening length and therefore Eq. (4) holds. The bond lengths for C_2^+ and CH^+ are from Refs. 50 and 51, respectively.

In this velocity domain, as mentioned in Sec. III A, atomic ions reach charge equilibrium within about 10 Å of the surface. The molecular ions are also expected to reach charge equilibrium near the surface. Maor *et al.*[34] found that for fast molecular ions, namely 4.2-MeV N_2^+ ions, the binding electrons are lost very rapidly, as with the atomic ions. Some differences between the molecular and atomic equilibration lengths were observed,[34] but the effects are too small to be important in the context of desorption.

2. *Secondary molecular-ion yields with incident molecular ions*

Desorption experiments have been performed using a number of different sets of incident molecular ions over a range of velocities. Three different compounds have been introduced into the ion source to produce the following primary molecular ions with energies ranging between 600 keV and 3.7 MeV: (1) CO_2 gas to produce C^+, O^+, CO^+, O_2^+, and CO_2^+; (2) Allene gas to produce C^+, CH^+, CH_3^+, C_2^+, C_3^+, and $C_3H_3^+$, and (3) a low-boiling-point perfluorokerosene liquid[52] volatilized to produce CF^+, CF_3^+, $C_3F_5^+$, and $C_4F_7^+$. Time-of-flight mass spectra of valine have been obtained using all of these incident ions over a range of different velocities. The mass spectra have features similar to those produced with atomic ions. The only differences occur in the relative magnitude of the secondary ion peaks.[28]

Figure 5 shows the measured yield of valine $(M\text{-H})^-$ ions measured as a function of the velocity of incident C^+, CH^+, CH_3^+, and C_2^+ ions. The existence of collective effects is evident when comparing the C_2^+ to the C^+ data. In the absence of collective molecular effects and considering the relation $Y \propto (dE/dx)^2$, it would be predicted that $Y(C_2^+) \sim 4Y(C^+)$, at the same velocity. However, the experimental results are $Y(C_2^+) \sim 8Y(C^+)$. As reported in Ref. 27, the data for C_3^+ also show strong nonlinearities, $Y(C_3^+) \sim 16Y(C^+)$.

The enhancement in the yield of CH^+ compared to C^+ (see Fig. 5) is much larger than expected. The ratio of the effective charges, q, of carbon to hydrogen (at 0.4 cm/ns) is about 3. Since $dE/dx \propto q^2$, the corresponding ratio of the stopping powers is about 9. Furthermore, since $Y \propto (dE/dx)^2$, the yield ratio of a proton compared to a carbon incident ion should be in the region of a few percent. Therefore, the secondary ion yield due to a proton at the same velocity would be smaller than the error bars for the C^+ data. Figure 5 shows clearly the effect of the extra proton on the yield of CH^+ (about 50% that of C^+). Furthermore, the increase in the yield from C^+ to CH_3^+ is larger than three times that from C^+ to CH^+.

Brandt *et al.*[17] have measured enhancements in electronic stopping power per atom for hydrogen clusters. The interpretation was that the electronic stopping power enhancement was due to the overlap of the electron polarization wakes left by the passage of the fast ions in the medium, referred to as the "vicinage" effect.[17] Tape *et al.*[18] also performed similar experiments with H_2^+ and O_2^- incident ions and obtained similar results. The enhancement in dE/dx was described by the electronic stopping-power enhancement factor R which is the ratio

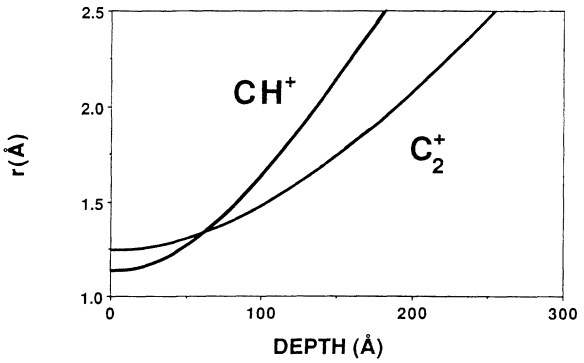

FIG. 4. The Coulomb explosion of CH^+ and C_2^+ ions at an incident velocity of 0.54 cm/ns. r (Å) is the distance between the constituent atoms and depth (Å) is the distance traveled by the primary molecular ion into the sample.

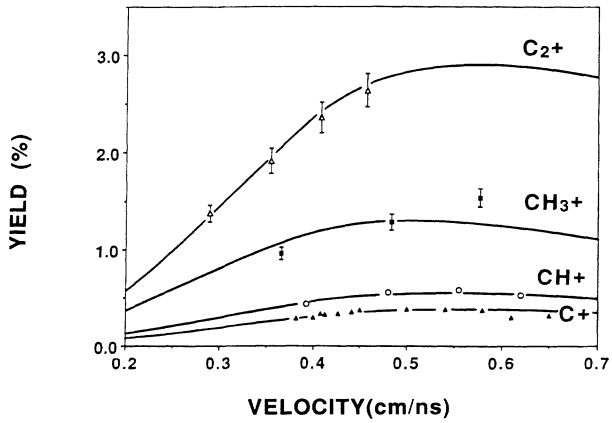

FIG. 5. The yield of valine $(M\text{-H})^-$ ions as a function of the velocity of incident C^+ (solid triangles), CH^+ (open circles), CH_3^+ (solid squares), and C_2^+ (open triangles). The fit to the data points is based on Eq. (6) and is discussed in the text.

of the stopping power of the molecular ion to that of the sum of its separate atomic constituents in the medium. Experimental results reported so far for R have been between 1–1.5.[17,18,53] For a heteronuclear molecular ion $X_n Y_m{}^+$ $(n,m=0,1,\ldots)R$ can be written as

$$R=\frac{\frac{dE}{dx}(X_n Y_m)}{\left[n\frac{dE}{dx}(X)+m\frac{dE}{dx}(Y)\right]}, \tag{5}$$

where $(dE/dx)(X)$ and $(dE/dx)(Y)$ are the electronic stopping power of the separate atomic constituents. Analogous to Eq. (3) for atomic ions, we have for the secondary ion yield with incident $X_n Y_m$ ions

$$Y(X_n Y_m)=KR^2\left[n\frac{dE}{dx}(X)+m\frac{dE}{dx}(Y)\right]^2. \tag{6}$$

The constant K is the same as that used for the atomic ions. From the fit to the atomic incident ions the constant K in Eq. (3) has been determined. The R values used in association with desorption will be effective values averaged over the desorption depth.

The fit to the data points for CH^+, $CH_3{}^+$, and $C_2{}^+$, shown in Fig. 5, are for R values of 1.11, 1.40, and 1.39, respectively. The fit to the C^+ data is also shown in Fig. 5. There are no literature R values for CH^+ and $CH_3{}^+$ ions, but the R value for $C_2{}^+$ ions is approximately the same as that reported for incident $O_2{}^-$ incident ions in the same velocity region.[18]

Figure 6 shows the yield of valine $(M\text{-H})^-$ ions as a function of the velocity of the incident C^+, O^+, CO^+, $O_2{}^+$, and $CO_2{}^+$ ions. The fit to the data points for the atomic ions was done using Eqs. (1)–(3), as described in Sec. III A, using the same K value. Assuming a simple additive stopping power for the stopping power of CO^+ and the $Y\propto(dE/dx)^2$ relation, we would expect $Y(CO^+)\sim 5Y(C^+)$. However, the measured values are much larger, i.e., $Y(CO^+)\sim 9Y(C^+)$. Making similar assumptions for $O_2{}^+$ incident ions one would expect $Y(O_2{}^+)\sim 4Y(O^+)$ which is considerably smaller than the measured value of $Y(O_2{}^+)\sim 7Y(O^+)$. The same reasoning applied to $CO_2{}^+$ incident ions would give an expected $Y(CO_2{}^+)\sim 13Y(C^+)$ whereas the measured value is roughly 22 times that of C^+ incident ions at the same velocity. Therefore, the incident molecular ions exhibit collective effects on the desorption yields, beyond that expected by a $Y\propto(dE/dx)^2$ relation. The fits to the CO^+, $O_2{}^+$, and $CO_2{}^+$ incident ion data are based on Eq. (6) giving $R=1.32$ in each case.

Figure 7 shows the yield of valine $(M\text{-H})^-$ ions as a function of the velocity of C^+, CF^+, $CF_3{}^+$, $C_3F_5{}^+$, and $C_4F_7{}^+$ incident ions. As with other incident molecular ions, collective molecular effects exist for these molecular ions. The fit to the data points for CF^+, $CF_3{}^+$, $C_3F_5{}^+$, and $C_4F_7{}^+$ are based on Eq. (6) for $R=1.39$. The combination of the $Y\propto(dE/dx)^2$ relation and the collective effects give rise to very high yields with the larger incident ions (Fig. 7). The highest yields, obtained with 2-MeV $C_4F_7{}^+$ and 2.8-MeV $C_3F_5{}^+$, are more than a factor of 60 higher than the slowest carbon ions (600 keV). Such high yields could be quite useful in the applied field of mass spectrometry, in particular for the desorption of large organic molecules.

Håkansson *et al.*[16] have shown for a number of organic samples that the secondary molecular-ion yields behave nonlinearly with respect to the electronic stopping power of the incident atomic ions below a certain "threshold" dE/dx. Above this value of dE/dx, the yield becomes linear with respect to dE/dx. This effect may explain the reason the fits to the data points are not very good for molecular ions with high stopping powers such as $CO_2{}^+$ ions in Fig. 6 and $CF_3{}^+$, $C_3F_5{}^+$, and $C_4F_7{}^+$ in Fig. 7.

3. *Electronic stopping of molecular ions*

Consider a molecular ion with an effective charge Q_{mol} and the separate atomic constituents at the same velocity

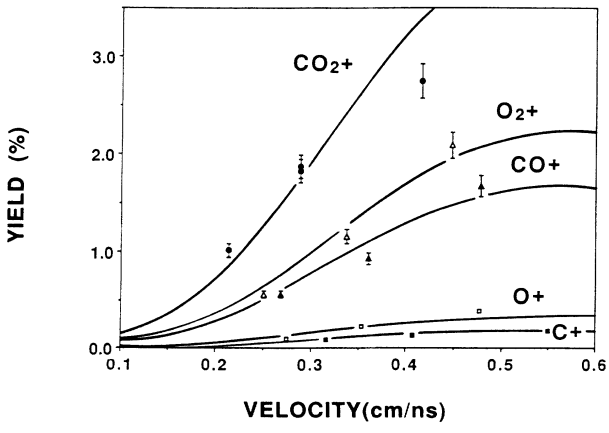

FIG. 6. The yield of valine $(M\text{-H})^-$ ions as a function of the velocity of incident C^+ (solid squares), O^+ (open squares), CO^+ (solid triangles), $O_2{}^+$ (open triangles), and $CO_2{}^+$ (solid circles). The fit to the data points is based on Eq. (6) and is discussed in the text.

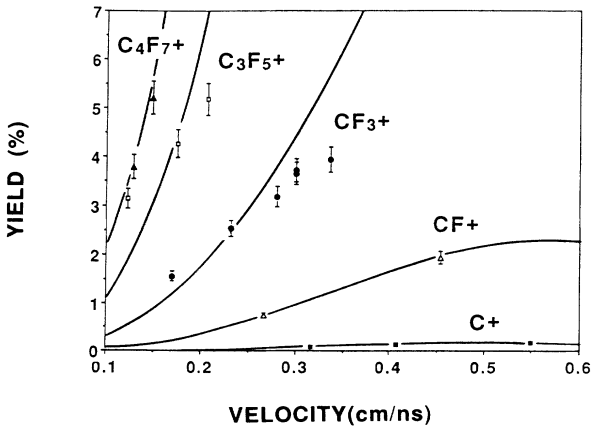

FIG. 7. The yield of valine $(M\text{-H})^-$ ions as a function of the velocity of incident C^+ (solid squares), CF^+ (open triangles), $CF_3{}^+$ (solid circles), $C_3F_5{}^+$ (open squares), and $C_4F_7{}^+$ (solid triangles). The fit to the data points is based on Eq. (6) and is discussed in the text.

having effective charges q_i. The effective charge of the molecule is between two limits,[17,49]

$$\sum_i (q_i)^2 < Q_{\text{mol}}^2 < \left[\sum_i q_i\right]^2 . \tag{7}$$

The lower limit corresponds to the constituent atoms being far enough apart (farther than the characteristic charge screening length) so that they can be treated as separate charges. The upper limit is the unified charge limit, experimentally unrealizable for molecular ions. From the yield data presented here, the relative dE/dx, and thus the relative effective charges of molecular ions with respect to the atomic constituents, can be determined. For example, in the simple case of C_2^+ incident ions, $Y(C_2^+) \sim 8Y(C^+)$. Therefore, $Q_{C_2}^2 \sim \sqrt{8} q_c^2$ which, once substituted, satisfies inequality (7). For all the molecular ions used in this experiment, the corresponding effective charges obtained in the manner explained above satisfy relation (7).

Brandt *et al.*[17] described the collective effects in dE/dx as being due to the superposition of particles' electron polarization "wakes." As discussed by Bohr,[33] a fast ion traversing matter causes the polarization and collective displacement of the target electrons due to the strong electric field created by the passage of the ion. This cylindrically symmetric polarization, the so-called wake, acts as a brake on the ions. As shown by Vager and Gemmel[54] the stopping power derived by linear-response theory approximates well with the Bethe stopping-power formula[55] for atomic ions. The wake approach to the interaction of ions with solids immediately necessitates the introduction of the concept of plasmons, i.e., collective excitation of valence electrons. Plasmons are well understood in solid-state theory of metals where valance electrons facilitate density fluctuations. A number of experiments have shown the existence of plasma oscillations in solids such as carbon,[56] frozen xenon,[57] and aluminum.[57] Collective excitations in insulators have been addressed by a number of authors.[58–60] Measurements have shown the existence of collective electronic excitations in a variety of insulators such as DNA,[61] nucleic-acid bases,[62,63] water,[64] benzene,[65,66] polyethylene,[67] and hydrocarbons.[68]

Arista,[69] in a similar approach to that of Ref. 17, assumed a one-dimensional charge density created by the passage of diatomic molecular ions, from which, using Poisson's equation, the induced electric field was calculated. This electric field acts as the braking force which gives rise to the stopping power. The collective effects of cluster ions arise from the superposition of the electric fields induced by the passage of the atoms in the cluster. The Lindhard's electron gas dielectric approximation at high velocities ($v > v_0$) was used. Arista derived an expression for the electronic stopping-power enhancement factor for a dicluster,

$$R = 1 + \left[\frac{2q_1 q_2}{q_1^2 + q_2^2}\right] \frac{I}{L} , \tag{8}$$

where q_1 and q_2 are the effective charges for the constituent atoms and

$$I = (1-\gamma) + \ln\left[\frac{v}{r_0 \omega_p}\right] \tag{9}$$

and

$$L = \ln\left[\frac{2mv^2}{\hbar\omega_p}\right] , \tag{10}$$

where L also appears in the stopping-power expression for atomic ions in Bethe's formula,[55] I is the molecular interference term, $\hbar$ is Planck's constant, $\gamma = 0.577$ is Euler's constant, ω_p is the plasma frequency for the medium, m is the electron mass, and r_0 is the molecular bond length.

Equations (8)–(10) have been used to calculate the R value for a number of diatomic incident molecular ions. The bond length for CH^+, C_2^+, CO^+, and O_2^+ ions were obtained from Refs. 50, 51, 70, and 71, respectively. In the calculations for R, we have used an ω_p value of 20 eV which is from the literature on optical reflectance and transmission measurements. As a rule, organic materials have ω_p values of about 20 eV.[60] Examples are DNA,[61] nucleic-acid bases,[62,63] and polyethylene.[67] At a velocity of 0.4 cm/ns, the predicted R values are $R(CH) = 1.09$, $R(C_2) = 1.23$, $R(CO) = 1.27$, $R(O_2) = 1.18$, and $R(CF) = 1.23$. These predicted R values are within 15% of the experimentally fitted values. Considering that the measured R values here are obtained from desorption experiments and the fact that Arista's analytical solution is for an electron gas medium, the agreement is quite reasonable.

IV. SUMMARY AND CONCLUSIONS

A number of different atomic and molecular incident ions over an energy range of 600 keV–3.7 MeV have been produced and used as incident ions in desorption experiments. The desorption yield of secondary negative molecular ions from a sample of the amino acid valine (MW of 117) has been measured for different incident ions. The yields due to incident atomic ions obey a square dependence on the electronic stopping power, $Y \propto (dE/dx)^2$. The yields from molecular incident ions, as well as following the square dependence, show an additional collective behavior. This collective effect was observed for all incident molecular ions in these experiments. Such collective effects give rise to high yields of secondary molecular ions. The yield enhancement as a result of molecular-ion impact is explained as being due to enhancement in dE/dx per atom in an incident molecular ion. The enhancement in dE/dx per atom has been experimentally observed by others.[17,18] The electronic stopping-power enhancement factor R can be estimated using a theory developed by Arista.[69] The estimates agree to within 15% of the R values deduced from the experimental data for the molecular ions.

The large enhancements in the secondary ion yield produced by using incident molecular ions could be of great importance in the field of mass spectrometry. The absolute yield values obtained here for molecular ions are comparable to those obtained with fission fragments from

a ^{252}Cf source or ions from high-energy accelerators[16] (e.g., 90-MeV $^{127}I^{12+}$). This makes low-energy accelerators (few MeV) such as a Dynamitron suitable and possibly preferable for the study of very large secondary molecular ions. It has been shown[16,72] that strong nonlinearities of the secondary ion yields with respect to the electronic stopping power exist for high-molecular-weight organic samples (MW of over $2000u$). This nonlinearity becomes more pronounced for the larger secondary ions. Thus, molecular primary ions are ideally suitable for the study of high-molecular-weight secondary ions which are very important in the field of mass spectrometry. Such work is underway at this laboratory.

Finally, Salehpour *et al.*[10] have shown that electronic sputtering is mostly a neutral ejection process with the secondary ion fraction being about $1:10^4$. In experiments with incident 90-MeV $^{127}I^{12+}$ ions they reported total yields of about 1200 intact molecules for the amino acid leucine and valine. Based on the measurements of Brown *et al.*[24] on total yields of water ice and those of Hedin *et al.*[73] on the leucine neutral, positive, and negative secondary ion yields, it is expected that the collective effects shown here for secondary ions would also exist for the total yield.

ACKNOWLEDGMENTS

The authors wish to express their gratitude to Professor Robert Johnson for reading the manuscript and making invaluable suggestions. We thank Dr. Elliot Kanter and Dr. Ali Belkacem for many fruitful and interesting discussions. The Dynamitron staff, Art Ruthenberg, Ron Amrein, and Bruce Zabransky, are gratefully acknowledged for their support and patience. Work performed under the auspices of the Office of Basic Energy Sciences, U.S. Department of Energy under Contract No. W-31-109-ENG-38.

---

*Present address: Department of Radiation Sciences, Ion Physics Division, Box 535, Uppsala University, 751 21 Uppsala, Sweden.

†Permanent address: Kent State University, Department of Chemistry, Kent, Ohio 44242.

[1]P. Sigmund, Phys. Rev. **184**, 383 (1969).

[2]D. F. Torgerson, R. P. Skowronski, and R. D. Macfarlane, Biochem. Biophys. Res. Commun. **60**, 616 (1974).

[3]R. D. Macfarlane, C. J. McNeal, and J. E. Hunt, Adv. Mass Spectrom. **8A**, 349 (1980).

[4]Bio-Ion Nordic AB, P.O. Box 15045, S-750 15 Uppsala, Sweden.

[5]B. Sundqvist, P. Roepstorff, J. Fohlman, A. Hedin, P. Håkansson, I. Kamensky, M. Lindberg, M. Salehpour, and G. Säwe, Science **226**, 696 (1984).

[6]I. Kamensky and A. Craig (unpublished).

[7]P. Håkansson and B. Sundqvist, Radiat. Eff. **61**, 179 (1982).

[8]P. Dück, H. Frölich, W. Treu, and H. Voit, Nucl. Instrum. Methods **191**, 245 (1981).

[9]W. Knippelberg, O. Becker, and K. Wien, Nucl. Instrum. Methods **198**, 59 (1982).

[10]M. Salehpour, P. Håkansson, B. Sundqvist, and S. Widdiyasekera, Nucl. Instrum. Methods B **13**, 278 (1986).

[11]P. Håkansson, E. Jayasinghe, A. Johansson, I. Kamensky, and B. Sundqvist, Phys. Rev. Lett. **47**, 1227 (1981).

[12]W. Guthier, O. Becker, S. Della-Negra, W. Knippelberg, Y. LeBeyec, U. Weikert, K. Wien, P. Wieser, and R. Wurster, Int. J. Mass Spectrom. Ion Phys. **53**, 185 (1983).

[13]H. Voit, H. Fröhlich, P. Dück, B. Nees, E. Nieschler, W. Bischof, and W. Tiereth, IEEE Trans. Nucl. Sci. **NS-30**, 1759 (1983).

[14]G. Säwe, P. Håkansson, B. U. R. Sundqvist, R. E. Johnson, E. Söderström, and S. E. Lindquist, Appl. Phys. Lett. **51**, 1379 (1987).

[15]G. Säwe, P. Håkansson, B. U. R. Sundqvist, and U. Jönsson, Nucl. Instrum. Methods B **26**, 579 (1987).

[16]P. Håkansson, I. Kamensky, M. Salehpour, B. Sundqvist, and S. Widdiyasekera, Radiat. Eff. **80**, 141 (1984).

[17]W. Brandt, A. Ratkowski, and R. H. Ritchie, Phys. Rev. Lett. **33**, 1325 (1974).

[18]J. W. Tape, W. M. Gibson, J. Remillieux, R. Laubert, and H. E. Wegner, Nucl. Instrum. Methods **132**, 75 (1976).

[19]H. H. Andersen and H. L. Bay, J. Appl. Phys. **45**, 953 (1974).

[20]H. H. Andersen and H. L. Bay, J. Appl. Phys. **46**, 2416 (1975).

[21]S. S. Johar and D. A. Thompson, Surf. Sci. **90**, 319 (1979).

[22]S. S. Wong, R. Stoll, and F. W. Röllgen, Z. Naturforsch. **37a**, 718 (1982).

[23]A. D. Appelhans, J. E. Delmore, and D. A. Dahl, Anal. Chem. **59**, 1685 (1987).

[24]W. L. Brown, W. M. Augustyniak, E. Simmons, K. J. Marcantonio, L. J. Lanzerotti, R. E. Johnson, J. W. Boring, C. T. Reiman, G. Foti, and V. Pirronello, Nucl. Instrum. Methods **198**, 1 (1982).

[25]J. P. Thomas, P. E. Filpus-Luyckx, M. Fallavier, and E. A. Schweikert, Phys. Rev. Lett. **55**, 103 (1985).

[26]J. P. Thomas, A. Olapido, and M. Fallavier, in proceedings of the Fourth International Conference on Radiation Effects in Insulators, Lyon, France, 1987. [Radiat. Eff. (to be published)].

[27]M. Salehpour, D. L. Fishel, and J. E. Hunt, J. Appl. Phys. **64**, 831 (1988).

[28]M. Salehpour, D. L. Fishel, and J. E. Hunt, Int. J. Mass Spectrom. Ion Proc. **84**, R7 (1988).

[29]M. Salehpour, D. L. Fishel, and J. E. Hunt, Rap. Commun. Mass Spectrom. **2**, 59 (1988).

[30](a) E. Brunnix and G. Rudstam, Nucl. Instrum. Methods **13**, 131 (1961); (b) C. J. McNeal, R. D. Macfarlane, and E. L. Thurston, Anal. Chem. **51**, 2036 (1979).

[31]H. P. Garnir, P. D. Dumont, and Y. Baudinet-Robinet, Nucl. Instrum. Methods **187**, 625 (1981).

[32]E. Jayasinghe, P. Håkansson, I. Kamensky, B. Sundqvist, J. Fohlman, and P. Peterson, Tandem Accelerator Laboratory Report, No. TLU 82/81, University of Uppsala, Sweden (unpublished).

[33]N. Bohr, K. Dan. Vidensk. Selsk. Mat.-Fys. Medd. **18**, No. 8, 1948.

[34]D. Maor, P. J. Conney, A. Faibis, E. P. Kanter, W. Koenig, and B. J. Zabransky, Phys. Rev. A **32**, 105 (1985).

[35]For a bibliography of experimental results, R. C. Dehmel, H. K. Chau, and H. Fleischmann, At. Data **5**, 232 (1973).
[36]A. B. Wittkower and H. D. Betz, J. Phys. B **4**, 1173 (1971).
[37]I. S. Dmitriev, V. S. Nikolaev, L. N. Fateeva, and Ya. A. Teplova, Zh. Eksp. Teor. Fiz. **42**, 16 (1962) [Sov. Phys.—JETP **15**, 11 (1962)].
[38]C. H. Sofield, N. E. B. Covern, J. Draper, L. Bridwell, J. M. Freeman, C. J. Woods, and M. Spencer-Harper, Nucl. Instrum. Methods **170**, 257 (1980).
[39]*Handbook of Stopping Cross Sections of Energetic Ions in All Elements,* Vol. 5 of *Stopping and Ranges of Ions in Matter,* edited by J. F. Ziegler (Pergamon, New York, 1980).
[40]L. C. Northcliffe and R. F. Schilling, Nucl. Data Tables **A7**, 233 (1970).
[41]J. F. Ziegler and J. P. Biersack, in *Treatise on Heavy-Ion Science,* edited by D. A. Bromley (Plenum, New York, 1985), Vol. 6.
[42]W. Brandt, in *Atomic Collisions in Solids,* edited by S. Datz, B. R. Appleton, and C. D. Moak (Plenum, New York, 1975), Vol. 1, p. 261.
[43]*Hydrogen Stopping Powers and Ranges in All Elements,* Vol. 3 of *The Stopping and Ranges of Ions in Matter,* edited by H. H. Andersen and J. F. Ziegler (Pergamon, New York, 1977).
[44]H. D. Betz, Rev. Mod. Phys. **44**, 465 (1972).
[45]S. Della-Negra, O. Becker, R. Cotter, Y. LeBeyec, B. Monart, K. Standing, and K. Wien, J. Phys. (Paris) **48**, 151 (1987).
[46]O. Becker, S. Della-Negra, Y. LeBeyec, and K. Wien, Nucl. Instrum. Methods B **16**, 321 (1986).
[47]S. Della-Negra, D. Jacquet, I. Lorthiois, Y. Le Beyec, O. Becker, and W. Wien, Int. J. Mass Spectrom. Ion Phys. **53**, 215 (1983).
[48]P. Dück, H. Fröhlich, W. Treu, and H. Voit, Nucl. Instrum. Methods **191**, 245 (1981).
[49]W. Brandt and R. H. Ritchie, Nucl. Instrum. Methods **132**, 43 (1976).
[50]K. Kitaura, C. Satoko, K. Morokuma, Chem. Phys. Lett. **65**, 206 (1979).
[51]R. P. Sakon, K. Kirby, and B. Liu, J. Chem. Phys. **73**, 1873 (1980).
[52]PCR Research Chemicals, P.O. Box 1778, Gainsville, Florida.
[53]Y. Horino, M. Renda, and K. Morita, in Proceedings of the 12th International Conference on Atomic Collisions in Solids Okayama, Japan, 1987 [Nucl. Instrum. Methods (to be published)].
[54]Z. Vager and D. S. Gemmel, Phys. Rev. Lett. **37**, 1352 (1976).
[55]H. A. Bethe, Ann. Phys. (Leipzig) **5**, 325 (1930).
[56]E. T. Taft and H. R. Philipp, Phys. Rev. **138**, A197 (1965).
[57]H. Raether, *Springer Tracts in Modern Physics* (Springer, Berlin, 1965), Vol. 38, p. 84.
[58]W. Brandt and R. H. Ritchie, *Physical Mechanisms in Radiation Biology,* edited by R. D. Cooper and R. W. Wood [National Technical Information Center, Office of Information Services, United States Dept. of Commerce, Springfield, Virginia 22151, No. (CONF-721001, 1974)].
[59]N. M. March and M. Parrinello, *Collective Effects in Solids and Liquids,* edited by D. F. Brewer (University of Sussex, Hilger, Bristol, UK 1982).
[60]M. Inokuti, *Applied Atomic Collision Physics,* edited by S. Datz (Academic, New York, 1983), Vol. 4.
[61]T. Inagaki, R. N. Hamm, and E. T. Arakawa, J. Chem. Phys. **61**, 4246 (1974).
[62]M. Isaacson, J. Chem. Phys. **56**, 1813 (1972).
[63]L. C. Emerson, M. W. Williams, I. Tang, R. N. Hamm, and E. T. Arakawa, Radiat. Res. **63**, 235 (1975).
[64]J. M. Heller, Jr., R. N. Hamm, R. D. Birkhoff, and L. R. Painter, J. Chem. Phys. **60**, 3483 (1974).
[65]M. W. Williams, R. A. MacRae, R. N. Hamm, and E. T. Arakawa, Phys. Rev. Lett. **22**, 1088 (1969).
[66]U. Killat, Z. Phys. **262**, 83 (1973).
[67]L. R. Painter, E. T. Arakawa, M. W. Williams and J. C. Ashley, Radiat. Res. **83**, 1 (1980).
[68]G. Bissinger, J. Gaiser, J. M. Joyce, and M. Numan, Phys. Rev. Lett. **55**, 197 (1985).
[69]N. R. Arista, Phys. Rev. B **18**, 1 (1978).
[70]R. C. Sahni and B. C. Sawhney, Trans. Faraday Soc. **2**, 64 (1968).
[71]N. H. F. Beebee, E. W. Thulstrup, and A. Andersen, J. Chem. Phys. **64**, 2080 (1976).
[72]A. Hedin, P. Håkansson, B. Sundqvist, and R. E. Johnson, Phys. Rev. B **31**, 1780 (1985).
[73]A. Hedin, P. Håkansson, M. Salehpour, and B. Sundqvist, Phys. Rev. B **35**, 7377 (1987).

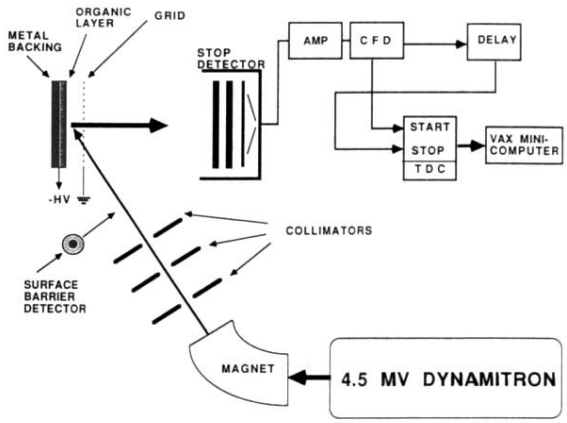

FIG. 1. The schematic diagram of the experimental setup. Abbreviations used are, amplifier (AMP), constant fraction discriminator (CFD), and time-to-digital converter (TDC).